Supplementary Material
Neuron, Volume 56

Release-dependent variations in synaptic latency: a putative code for short- and long-term synaptic dynamics

[1,2]Sami Boudkkazi, [1,2]Edmond Carlier, [1,2]Norbert Ankri, [1,2]Olivier Caillard, [1,2]Pierre Giraud, [1,2]Laure Fronzaroli-Molinieres & [1,2]Dominique Debanne°

[1]*INSERM U641, Marseille, F-13916 France*
[2]*Université de la Méditerranée, Faculté de Médecine secteur nord, IFR 11, Marseille, F-13916 France*

°To whom correspondence should be addressed,
Tel: (+33) 4 91 69 87 45
Fax: (+ 33) 4 91 09 05 06
E-mail: dominique.debanne@univmed.fr

Figure S1. Signal analysis method.

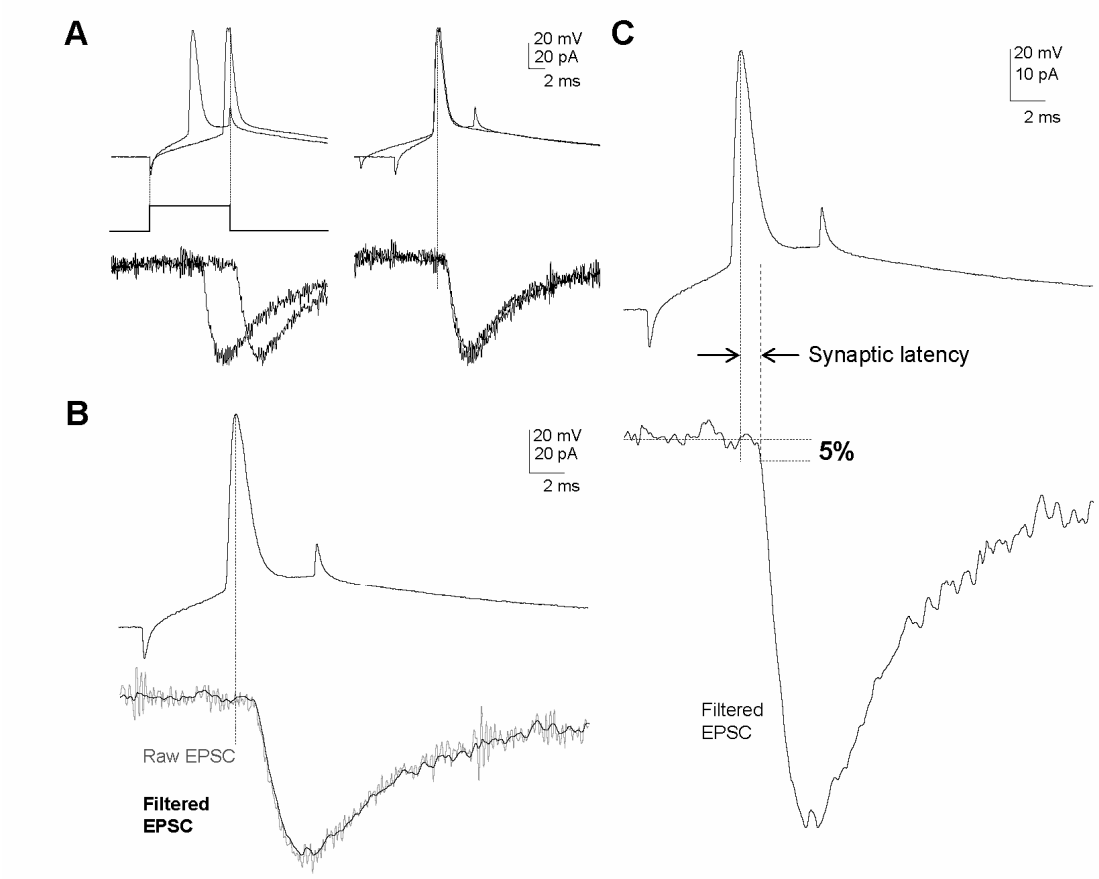

(**A**) Realignment of pre- and post-synaptic signals on the peak of the presynaptic AP. Right, aligned signals. (**B**) Filtering of post-synaptic currents. (**C**) Automatic measurement of synaptic latencies on filtered EPSCs.

Figure S2. Evaluation of the variation in latency due to propagation of the action potential in the axon.

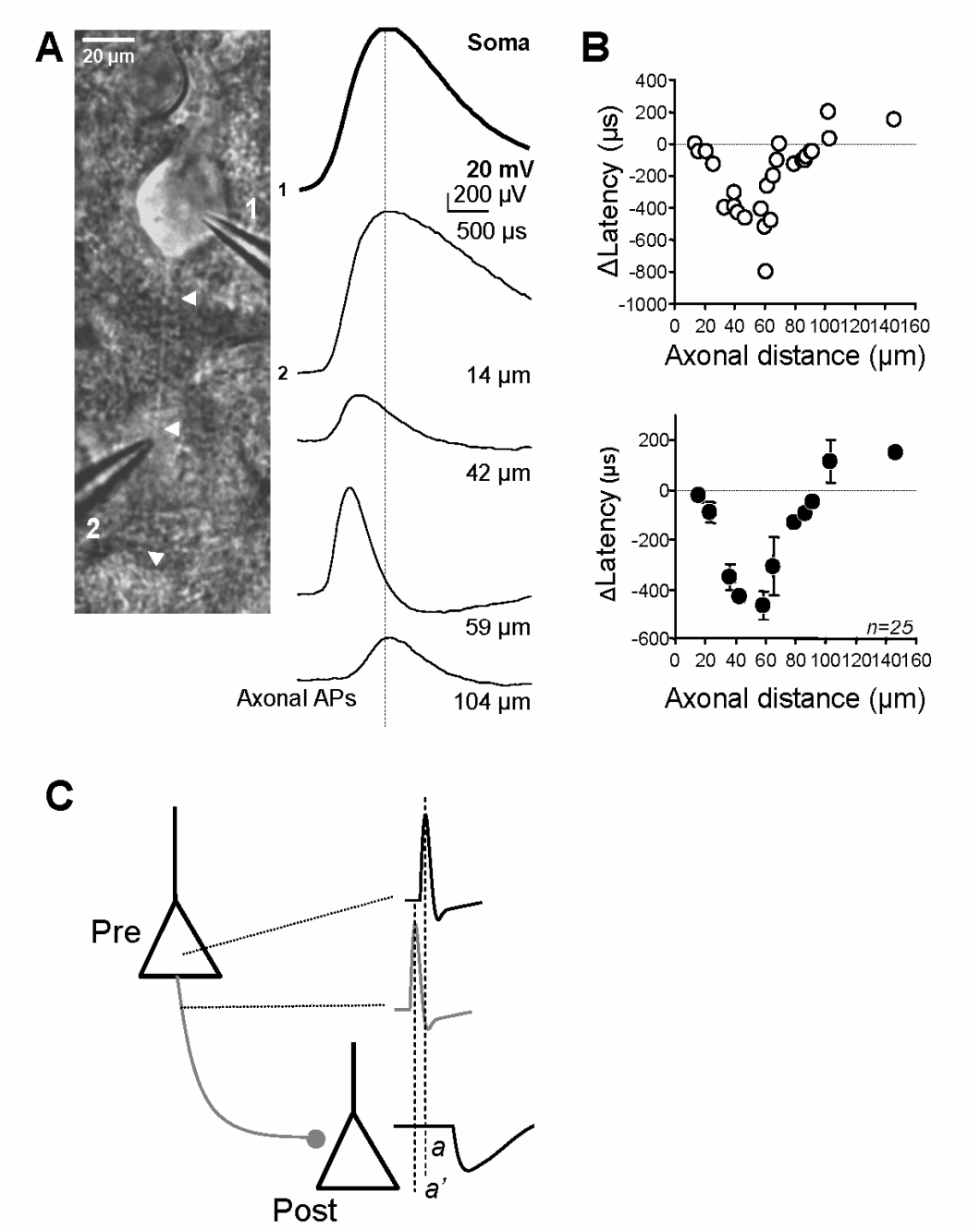

L5 pyramidal neurons were recorded in whole-cell configuration at the soma and in loose-patch configuration at the axon. (**A**) The variation in latency (ΔLatency) was measured as a function of the axonal recording distance on different neurons. The axonal AP recorded at 40-60 µm preceded the somatic AP but not at shorter or longer distances, indicating that the AP was initiated in the proximal region of the axon. (**B**) Quantification of the ΔLatency as a function of the axonal recording distance on 25 soma-axon pairs. (**C**) Axonal initiation and estimation of synaptic latency. Synaptic latency measured from the presynaptic AP measured in the soma (*a*) is shorter than that measured from the AP measured at ~50 µm from the soma (*a'*).

Figure S3. Effect of noise on latency measurement.

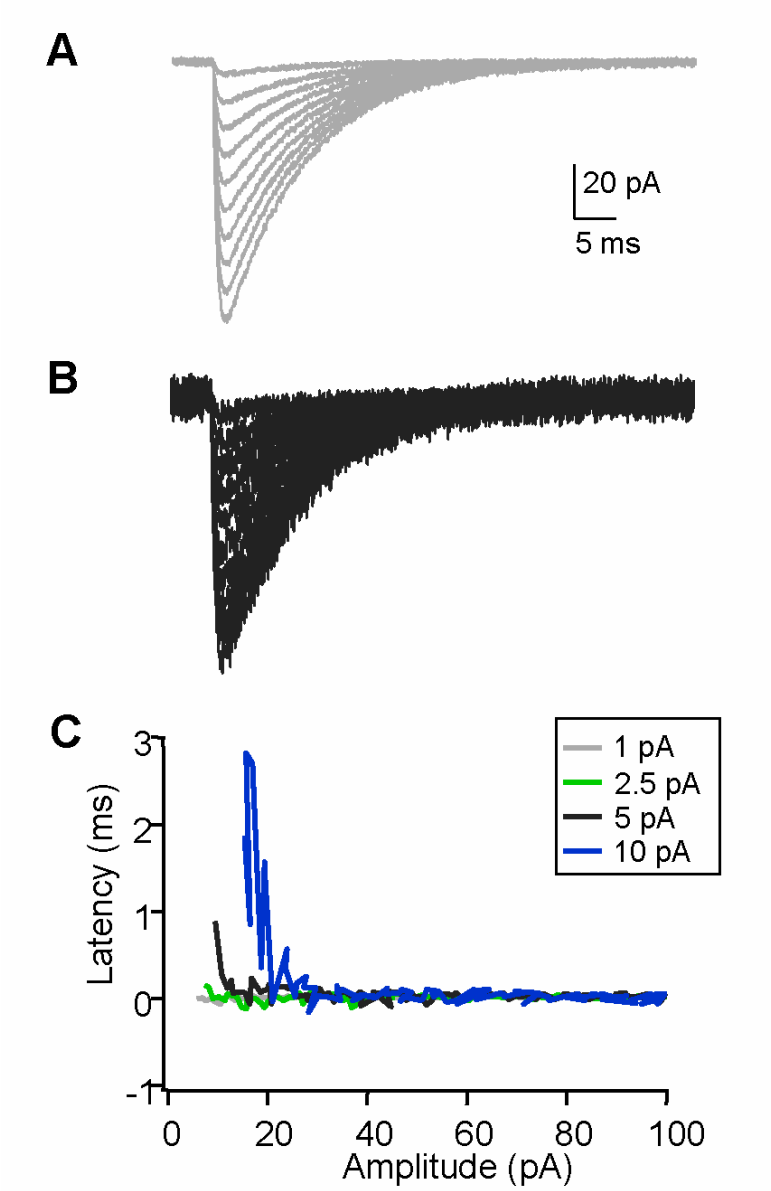

The possible erroneous measurement of latencies for small EPSCs was evaluated with simulated noisy EPSCs generated and analyzed with IgorPro 5 software. An EPSC template was generated according to the function $I_{EPSC} = I.\exp(1-\tau/\tau_{on}).\exp(-\tau/\tau_{off})$ with $\tau_{on} = 0.5$ ms and $\tau_{off} = 10$ ms with I_{EPSC} being 100 pA at maximum amplitude. From that template a scaling factor was applied to generate a broad range of EPSC amplitudes. Different levels of Gaussian noise (1-10 pA range) were then added to the simulated EPSCs. **(A)** Superimposition of 10 scaled EPSCs with 1 pA noise. **(B)** Superimposition of 10 scaled EPSCs with 5 pA noise. **(C)** Plot of latency (time at 5% of EPSC amplitude) *vs.* amplitude for scaled EPSCs with different levels of noise (1 pA, grey; 2.5 pA, green; 5 pA, black; 10pA, blue). Note that the measurement of latency remains accurate for all signal-to-noise ratios greater than 2-3.

Figure S4. Release probability determines the latency of compound EPSPs at L5-L5 connections.

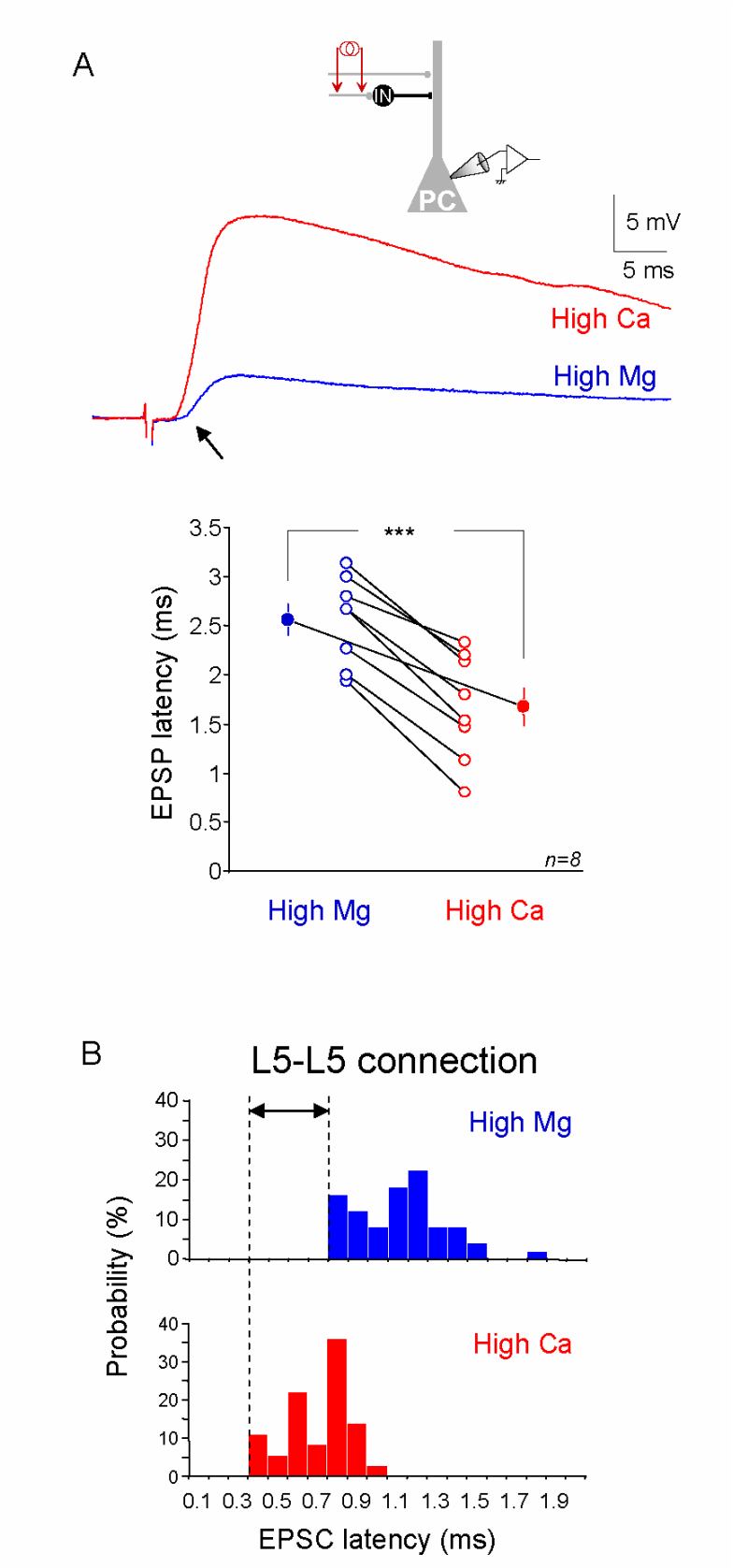

(**A**) Top, recording configuration. Middle, averaged traces (n=5) recorded in a saline containing a high concentration of Ca^{2+} (5 mM Ca^{2+}, 0.5 mM Mg^{2+}, red) or in a saline containing a high concentration of Mg^{2+} (3 mM Mg^{2+}, 1 mM Ca^{2+}, blue). Note the difference in latency (arrow). Bottom, quantification. The synaptic latency of the compound EPSP was significantly shorter in the presence of a high concentration of Ca^{2+} (1.7 ± 0.2 vs. 2.6 ± 0.2 ms in high Mg^{2+}, n = 8; paired t-test, $p<0.05$ (***)). (**B**) Distribution of EPSC latency in a representative L5-L5 connection in high Mg (top) and high Ca (bottom). Note the delay between the first latency bins (horizontal double arrow).

Figure S5. Quantal content determines subsequent release at L5-L5 connections.

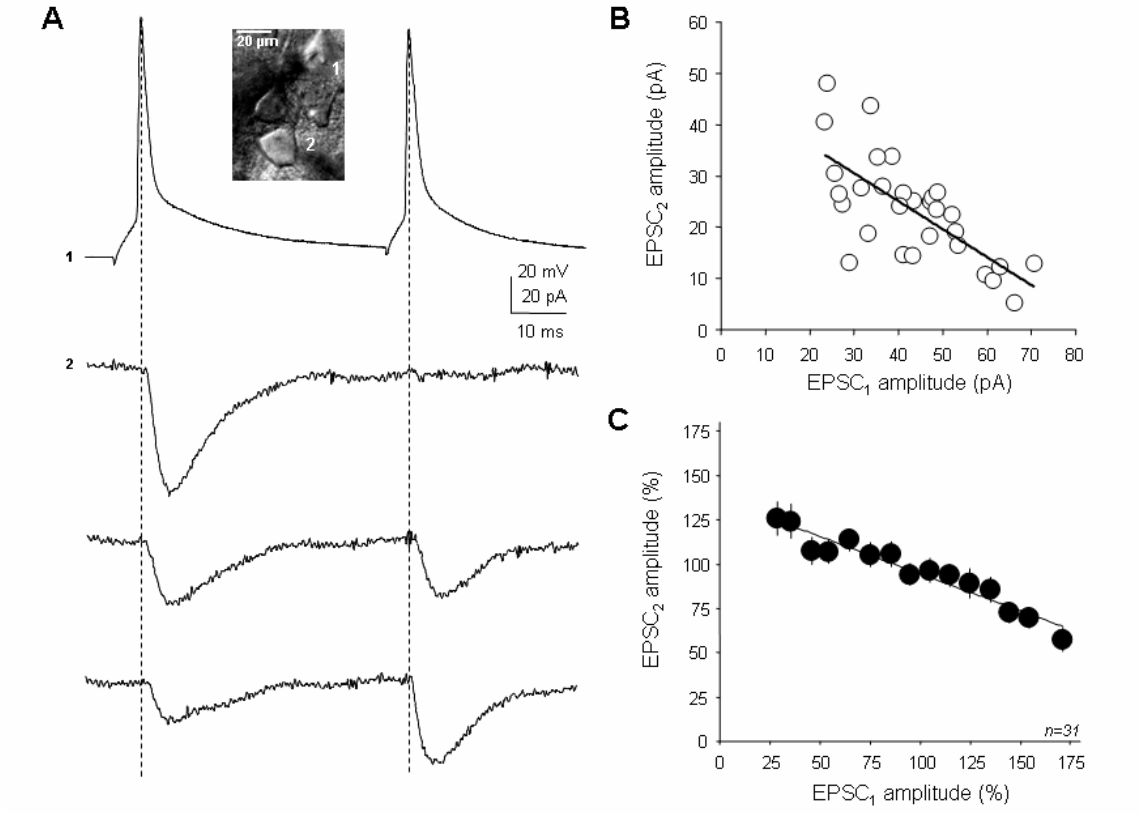

(**A**) & (**B**) Inverse correlation at a synaptic connection. Representative traces (A) and plot of $EPSC_2$ vs. $EPSC_1$ amplitudes (B, y = -0.5x + 46.8 R^2=0.50). (**C**) Pooled data over 31 connections (y = -0.4x + 134.6; R^2=0.93).

Figure S6. Release-dependent latency at L5-L5 EPSPs. In these experiments both pre- and post-synaptic neurons were recorded in current clamp.

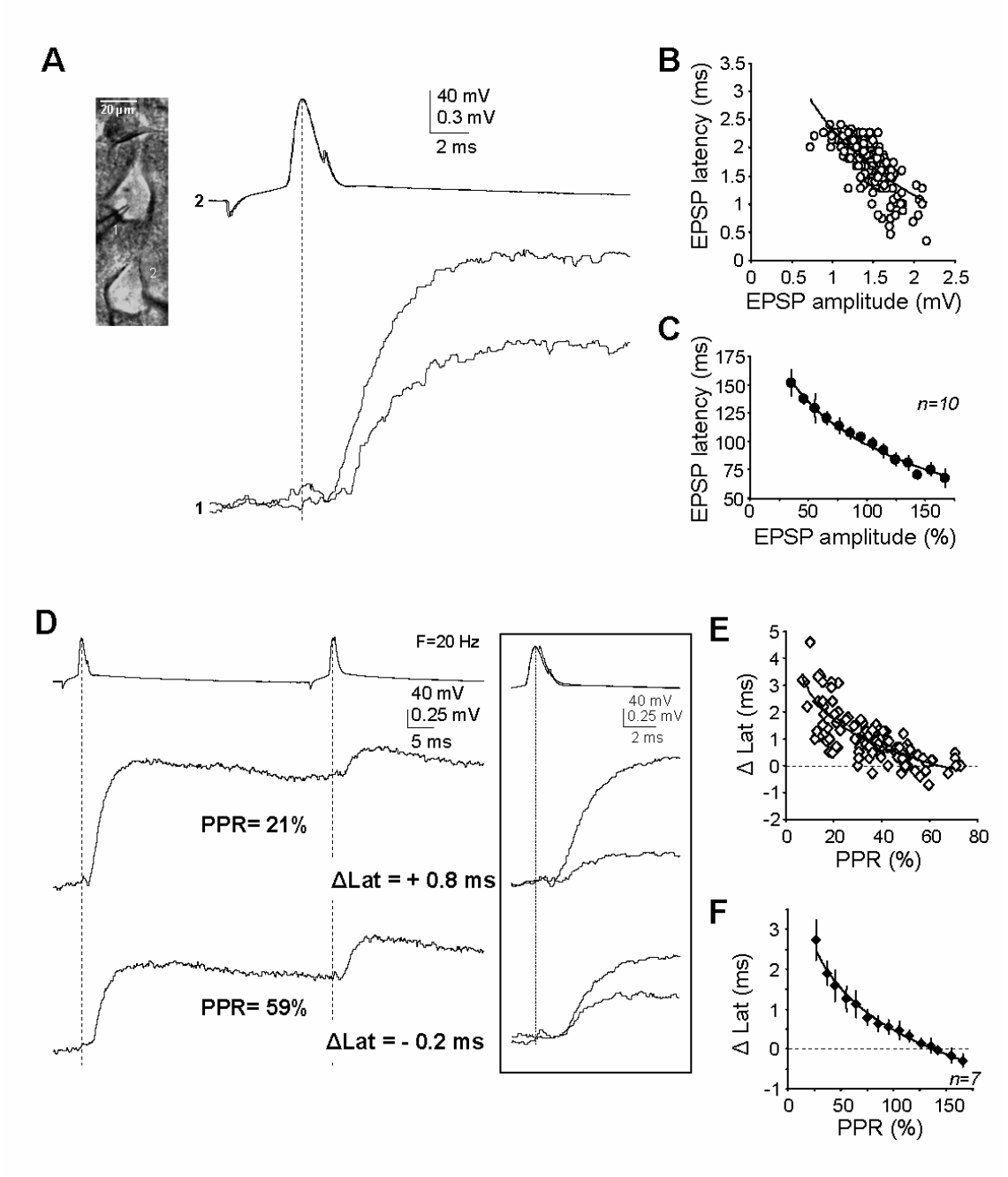

(**A**) amplitude-dependent latency in a single L5-L5 connection. (**B**), EPSP latency vs. EPSP amplitude. (**C***)*, Pooled data over 10 pairs (regression y= -54.2Ln(x) + 347, R^2=0.99). (**D**), Paired-pulse ratio determines the variation in latency. (**E**), Variation in latency (ΔLat) vs. paired-pulse ratio. (**F***)*, Pooled data of 7 pairs (regression: y = -1.514Ln(x) + 7.45, R^2=0.98)).

Figure S7. Effects of *Pr* on synaptic latencies during short-term plasticity at L5-L5 connections.

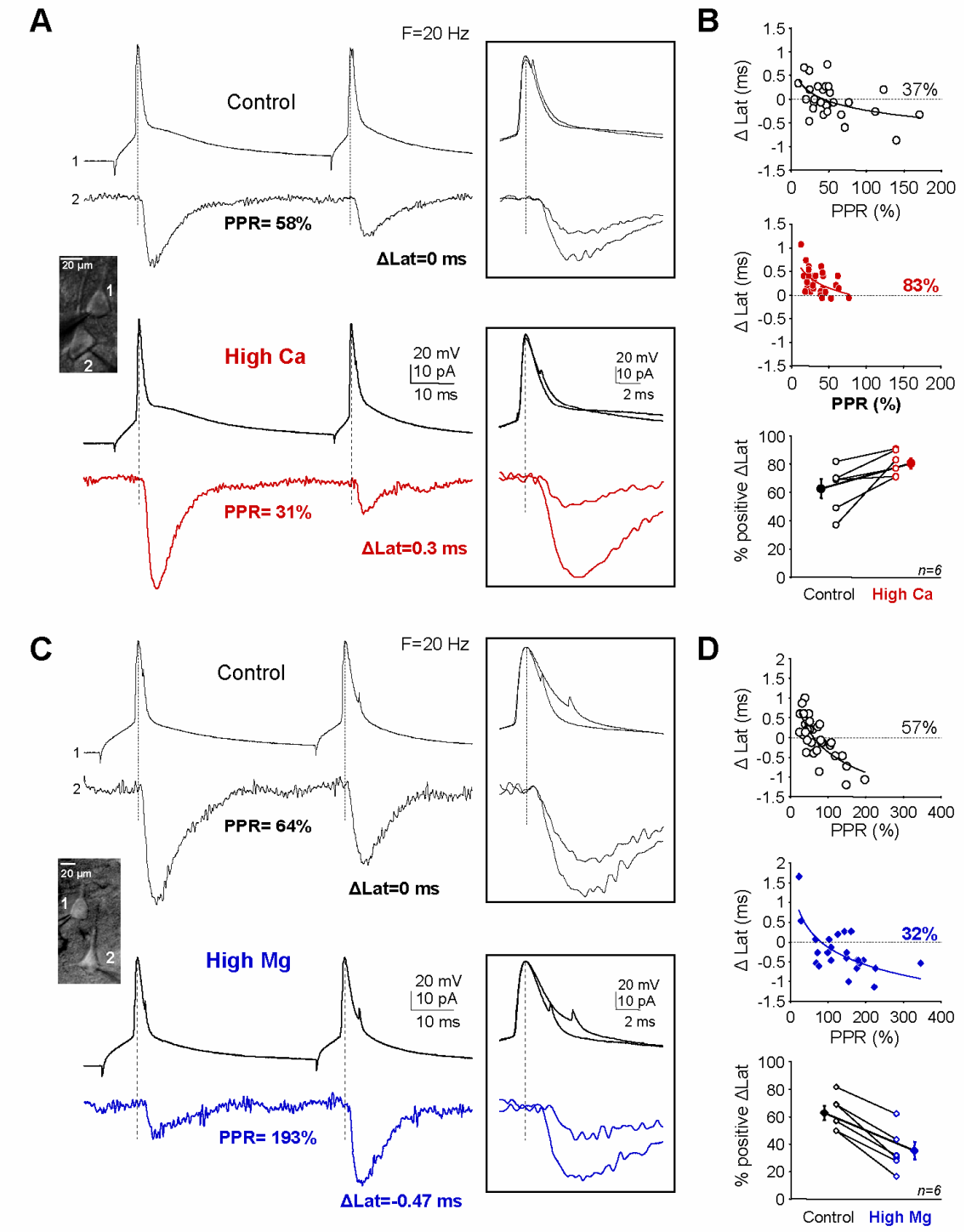

(**A**) and (**B**), effects of increasing *Pr* on PPR and synaptic latencies. Increasing the extracellular $[Ca^{2+}]$ to $[Mg^{2+}]$ ratio (from 3 mM Ca^{2+} and 2 mM Mg^{2+} (control) to 5 mM Ca^{2+} and 0.5 mM Mg^{2+}(High Ca)) decreased the PPR (A) and enhanced the percentage of trials exhibiting a positive ΔLat (from 37 to 83%, B). **(B)** Upper plots, ΔLat vs. PPR in control (○, y = -0.28Ln(x) + 1.05; R^2=0.24) and in High Ca (●, y = -0.31Ln(x) + 1.35; R^2=0.27). Bottom plot, summary of 6 experiments. (C) and (D), effects of decreasing *Pr* on PPR and synaptic latencies. Decreasing the extracellular $[Ca^{2+}]$ to $[Mg^{2+}]$ ratio (from 3 mM Ca^{2+} and 2 mM Mg^{2+}

(control) to 1 mM Ca^{2+} and 3 mM Mg^{2+}(High Mg), B) enhanced the PPR (C) and decreased the percentage of trials exhibiting a positive ΔLat (from 57 to 32%, D). (**D**), Upper plots, ΔLat vs. PPR in control (○, y = -0.75Ln(x) + 3.09; R^2=0.592) and in High Mg (●, y = -0.64Ln(x) + 2.82; R^2=0.5).Bottom plot, summary of 6 experiments.

Figure S8. Stability of axonal AP waveform during paired-pulse stimulation in L5 pyramidal neurons.

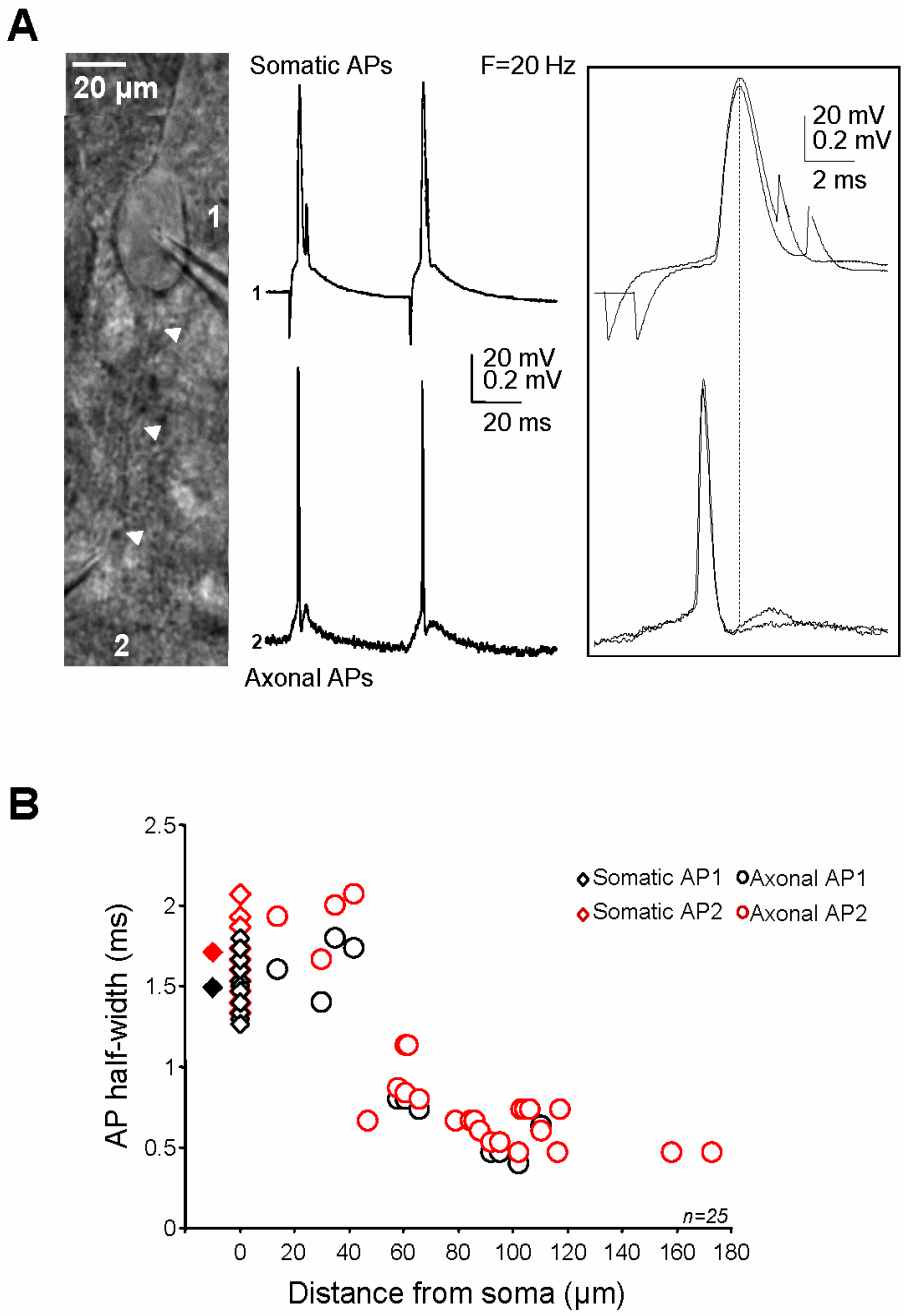

(A) Left, recording configuration: whole-cell patch-clamp recording at the soma (1) and cell-attached axonal recording at 80 µm (2). A pair of APs was elicited by current injection in the soma (ISI=50 ms). Inset, enlargement of the somatic and axonal APs. Note the broadening

at the soma but not at the axon. **(B)** Plot of AP half-width vs. the recording distance from the soma. Note that the difference between AP1 and AP2 seen at the soma disappears at 50-80 µm from the soma.

Figure S9. Release-dependent variations in latency at CA3-CA3 connections.

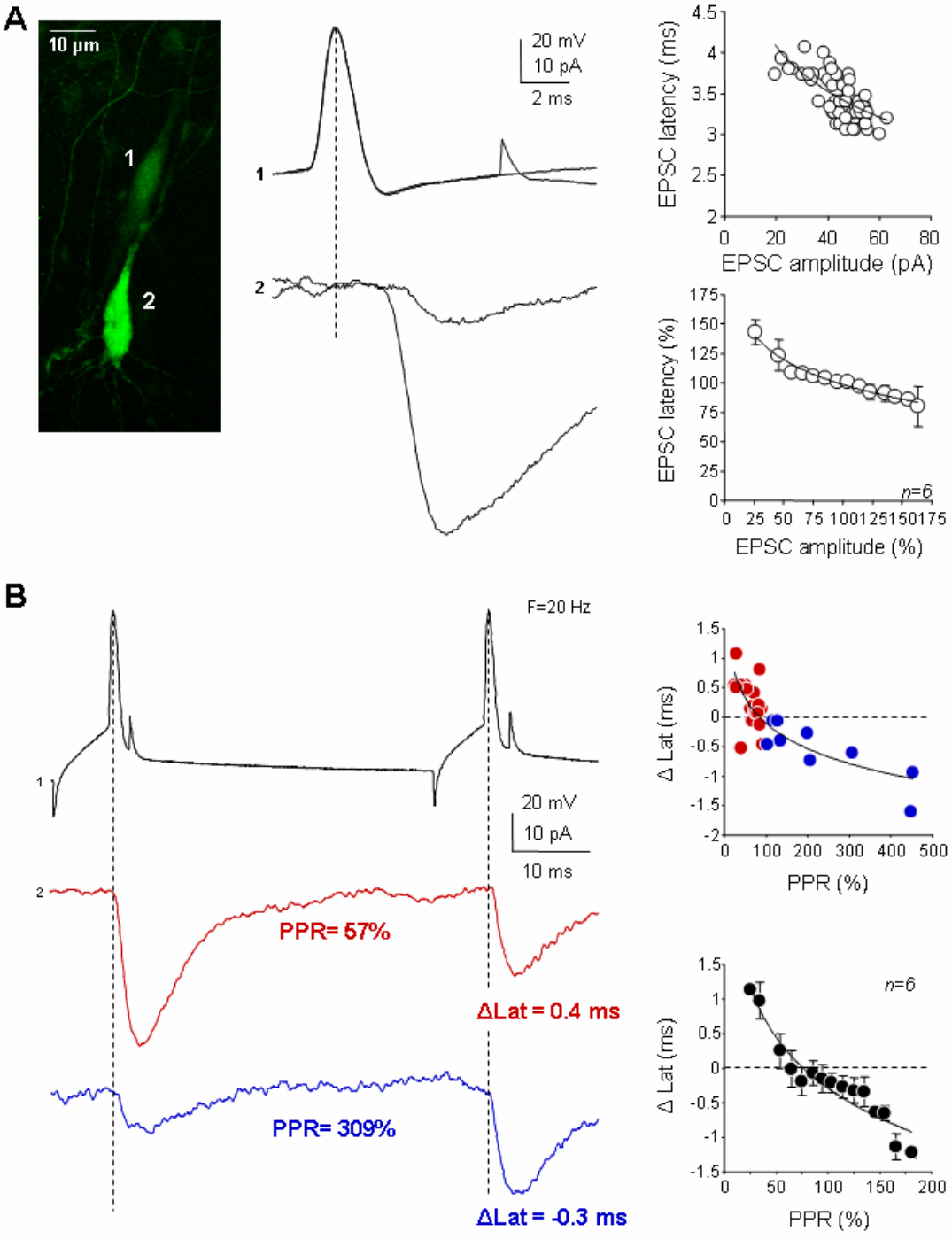

(**A**) Confocal reconstruction of a monosynaptically connected pair of CA3 pyramidal cells labelled with biocytin (left). Amplitude-dependent latency variations at a synapse formed by two CA3 pyramidal neurons. Middle, representative presynaptic action potentials (1) and evoked postsynaptic currents (2). Top right, EPSC latency vs. EPSC amplitude (y=-0.8 Ln(x)

+ 6.4 ; R^2=0.47). Bottom right, normalized pooled data over 6 CA3-CA3 synapses (y= -30.6 Ln(x) + 239.7; R^2=0.97). (**B**) Synaptic latency during short-term synaptic plasticity tested with pairs of presynaptic APs (ISI=50 ms). Positive synaptic latency difference (ΔLatency) is associated with PPD (upper traces) whereas negative synaptic ΔLatency is associated with PPF (bottom traces). Upper right, plot of ΔLatency as a function of the PPR (y=-0.59Ln(x) + 2.70; R^2=0.50). Lower right, pooled data over 6 CA3-CA3 synapses (y=-1.07Ln(x) + 4.62; R^2=0.92).